Hiroshima J. Med. Sci.
Vol. 72, No. 1·2, 11~19, June, 2023
HIMJ 72–3

Gradient magnetic-oscillation topography depicts high-frequency oscillations on the brain surface related to the epileptic focus in intractable epilepsy with lesions

Akitake OKAMURA[1,2)], Akira HASHIZUME[1,2)], Kota KAGAWA[1,2)], Masaya KATAGIRI[1,2)], Go SEYAMA[1,2)], and Koji IIDA[1,2,*)]

1) Department of Neurosurgery, Graduate School of Biomedical and Health Sciences, Hiroshima University, Hiroshima, Japan
2) Epilepsy Center, Hiroshima University Hospital, Hiroshima, Japan

ABSTRACT

This study aimed to evaluate high-frequency oscillations (HFOs), a potential biomarker of epileptic activity, using magnetoencephalography (MEG). We developed a new spatial filter, termed "gradient magnetic-oscillation topography" (GMOT), to visualize color-coded topographies on the brain surface using a spectrogram calculated at each sensor level. We enrolled 15 patients with lesions and intractable neocortical epilepsy who underwent focal resection surgery and preoperative MEG. We compared GMOT findings with those of the equivalent current dipole (ECD) and resected area based on intracranial video-electroencephalography (IVEEG) or intraoperative electrocorticography (ECoG) with respect to seizure outcomes. We also calculated the proportion of the power of each sensor relative to the entire head at each frequency band. GMOT successfully visualized the high-power gradient magnetic field at the fast ripple band (FR band, 201–330 Hz) and detected the highest power at the FR band around the lesion in 13 of the 15 patients. The resected area included both clustered ECDs and the highest power in the FR band on GMOT in 9 of the 15 patients. The resected area had a statistically higher proportion of power as the frequency band increased in the HFO group ($p < 0.01$). We visualized high power in the FR band of the brain surface. The areas of highest power in the FR band were correlated with epileptic focus based on IVEEG and intraoperative ECoG.

Key words: *Epilepsy*, *High frequency oscillations*, *Magnetoencephalography*, *Time-frequency analysis*

INTRODUCTION

High-frequency oscillations (HFOs) have attracted attention as potential biomarkers for epileptic activity[1,6)]. In particular, the search for HFOs using subdural electrodes has been widely performed clinically[8,18)]. HFOs (usually 80 Hz or more) can be detected noninvasively on scalp electroencephalography (EEG) and magnetoencephalography (MEG)[19,24,26,27)]. HFOs are typically divided into two categories: ripple (80–200 Hz) and fast ripple (FR; 200–330 Hz) bands.

Equivalent current dipole (ECD) estimation is the primary analytical method for MEG in epilepsy[3,13)]. However, it has been difficult to apply ECD estimation to the analysis of HFOs because of the low signal-to-noise ratios of HFOs in MEG[9)]. Furthermore, it is challenging to visually inspect waves using spatial filters in the HFO band containing ten times or more waves than the normal frequency. A new method has recently been reported in which sensors related to HFOs can be identified[27)]. However, this method is relatively complicated, and mathematical processing discards sensors that are unrelated to HFOs. Therefore, a new method is desired that can visualize the power of HFOs at anatomically precise locations without any signal loss based on time-frequency analysis.

In this study, we developed a new spatial filter called gradient magnetic-oscillation topography (GMOT) to visualize the power of all sensors directly on the brain surface without the influence of examiner bias or non-physiological mathematical constraints to solve ill-posed inverse problems. Previously, we developed a spatial filter for temporal-spatial analysis termed gradient magnetic-field topography (GMFT), which can visualize the signal amplitude of all planar gradiometers directly on the brain surface without examiner bias or loss of signal[11,14,17)]. In this study, we converted the GMFT to the GMOT for time-frequency analysis.

GMOT consists of two steps: eigenvalue decomposition of measured data to increase the signal-to-noise ratio and visualization of color-coded topographies on the brain surface with a spectrogram calculated at each sensor level. This enables a straightforward evaluation of brain activity at arbitrary frequency bands.

Herein, we evaluated the power of the HFO band

* Corresponding author: Koji Iida, MD, PhD, Department of Neurosurgery, Graduate School of Biomedical & Health Sciences, Hiroshima University, 1-2-3 Kasumi, Minami-ku, Hiroshima 734-8551, Japan
Tel: +81-82-257-5227, Fax: +81-82-257-5229, E-mail: iidak@hiroshima-u.ac.jp

using the GMOT in patients who underwent resective surgery for intractable lesional and neocortical epilepsy. We compared GMOT findings with those of ECDs and the resected area based on intracranial video-electroencephalography (IVEEG) or intraoperative electrocorticography (ECoG) with respect to seizure outcomes. We hypothesized that GMOT can detect high power in the FR band on the brain surface related to epileptic focus.

MATERIALS AND METHODS

Patients

This retrospective study was approved by the Ethics Committee of Hiroshima University, Japan (ethical approval E-749). We retrospectively reviewed the clinical records and preoperative MEG findings of patients with intractable lesional and neocortical epilepsy who underwent resective surgery at Hiroshima University Hospital between January 2018 and January 2022. We excluded patients with no lesions or hippocampal sclerosis. We included patients who underwent comprehensive presurgical evaluations using MEG, scalp video-electroencephalography (SVEEG), magnetic resonance imaging (MRI), positron emission tomography with fluorine-18 fluorodeoxyglucose, and iodine-123 iomazenil single-photon emission computed tomography. All patients and their families provided written informed consent prior to surgery.

MEG recording

A Neuromag System (whole-head 306-channel; MEGIN, Helsinki, Finland) was used. The participants were instructed to rest on a bed with their eyes closed during the measurement and were evaluated using monitors. Simultaneous MEG, EEG, electrocardiography, and electrooculography were digitized at 1,000 Hz, and an international 10–20 EEG electrode system was employed. A total of 3 to 6 sessions of nearly 10-min recordings were obtained for each participant. Recordings from the magnetometer coils were not used for the subsequent analysis. Participants underwent MRI examination, whereby the brain voxels were extracted manually from the structural head MRI data, and an individual polygon mesh was created.

GMOT analysis

Recordings from the magnetometers were not used. We used MATLAB R2020b for the signal and image processing. To extract neuronal signals from miscellaneous noisy components, a singular-value decomposition filter was employed. This filter consists of three steps: calculation of the variance matrices of the recorded data, eigenvalue decomposition, and data reconstruction through the inclusion of the ten largest eigenvalues. This filter aims to increase the signal-to-noise ratio at higher frequency bands to remove sensor noise that could be considered normal distributions[16,22]. MEG data were processed using the above filter with 0.5-s intervals of nearly 1 s each. Using a short-time fast Fourier transform, we calculated a spectrograph, the square root of the sum of the power spectrum at the orthogonal gradiometer coils. We designed the GMOT to draw a topography similar to the GMFT[11]. Each sensor was projected into the polygon-meshed brain surface in the vertical direction to produce a color map of the brain surface, reflecting the power of the time frequency (Figure 1). The transverse and longitudinal powers of the mth pair of the planar gradiometer are denoted as p_{T_m} and p_{L_m}, respectively. The color value of the projected point is defined as follows:

$$p_{pr_m} = \sqrt{p_{T_m}^2 + p_{L_m}^2}$$

GMOTs were generated to visualize the power spectra of the sensors (Figure 2a). We visually examined the EEG and MEG waves band-pass filtered at 3–35 Hz and 201–330 Hz to exclude periods in which noise contamination was suspected (Figure 2b, c). The GMOT detected the area on the brain surface with the highest power and that over 800 $(fT/cm)^2/Hz$ through the temporal space in the FR band. We generated two-dimensional GMOTs with 0.5-s steps for 1 s for the delta band (0.5–3 Hz), theta band (4–7 Hz), alpha band (8–13 Hz), beta band (14–30 Hz), low gamma band (26–45 Hz), high gamma band (46–70 Hz), low HFO band (71–100 Hz), middle HFO band (101–200 Hz), and high HFO band (FR, 201–330 Hz) (Figure 2d). We also generated three-dimensional GMOTs and superimposed the ECDs to visually compare the two methods (Figure 2e). When the GMOT detected high power throughout in more than half of the examinations, we defined this as frequent high power. If GMOT detected high power throughout less than half of the examinations, we defined this as rare high power. We also visually examined empty-room MEG waves to verify noise contamination at 201–330 Hz.

Proportion of power relative to the whole head

To standardize the power of the GMOT at different frequency bands, we defined the proportion of each sensor's power relative to the entire head at each frequency band. The proportion of power relative to the entire head was defined as the power of a projected point divided by the sum of the powers of all projected points in any frequency band. When the sensor array consists of M pairs of planar gradiometers, the proportion of power of the mth pair of the planar gradiometer relative to the entire head is defined as

$$p_{pr_m} / \sum_{i=1}^{M} p_{pr_i}$$

We defined epileptic focus as the ictal onset zone identified by IVEEG or the epileptic zone identified by intraoperative ECoG. We then evaluated the power of the epileptic foci (Figure 2f).

ECD estimation

Recordings from the gradiometers were bandpass filtered at 3–35 Hz. We visually inspected the interictal magnetic epileptiform with reference to the EEG and

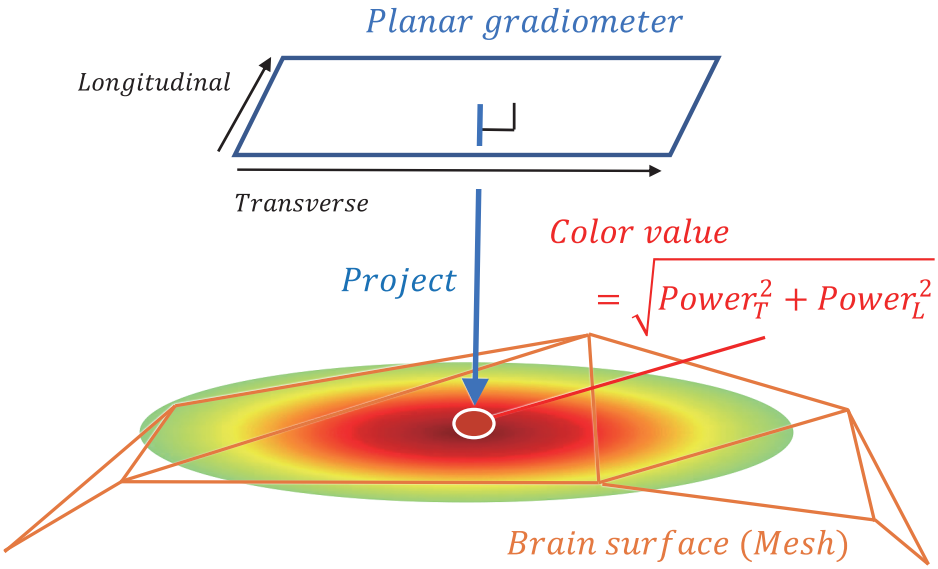

Figure 1 A schema for gradient magnetic-oscillation topography (GMOT) to assign colors to the brain surface as an indicator of power derived from the frequency band being analyzed. We calculated the square root of the sum of squares of the transverse and longitudinal powers detected by each planar gradiometer for the time frequency being analyzed ($Power_T$ and $Power_L$). The sensors were then projected onto the brain surface in the vertical direction for each sensor to apply a color map to the brain surface, reflecting the time frequency. To visualize FR, defined as the power from 201 to 330 Hz of 800 $(fT/cm)^2/Hz$ or higher, GMOT was generated for the frequency band, and the upper limit of the color map was set as 800 $(fT/cm)^2/Hz$.

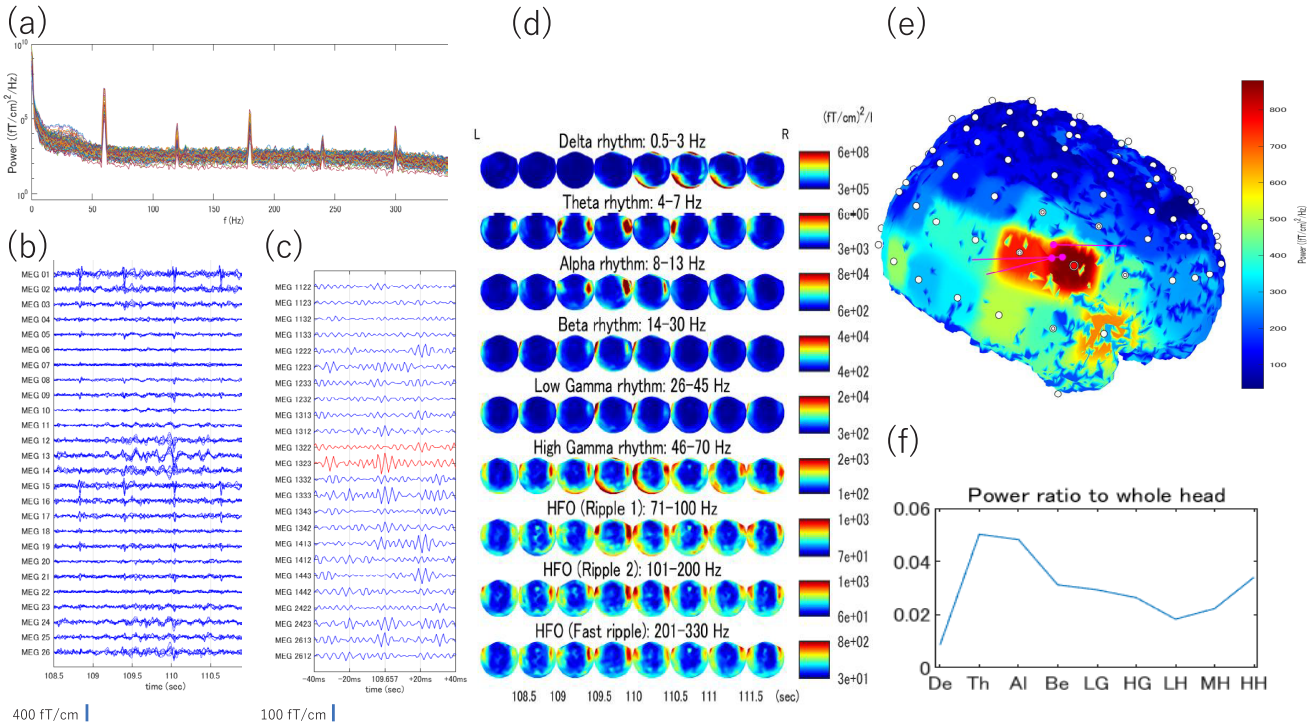

Figure 2 An example of GMOT analysis. (a) A power spectrum of the sensors from 108.5 to 112.5 s where a singular value decomposition filter is applied. (b) Raw waves at normal frequency with a MEG spike at 110.034 s. (c) Combined raw waves at the FR with high power at the MEG pair of 1332 and 1333. (d) Two-dimensional representation of GMOT (2D-GMOT). 2D-GMOTs of each frequency band show a spectrogram containing spatial information every 1 s. (e) Three-dimensional representation of GMOT (3D-GMOT). The 3D-GMOT at the FR from 109.5 to 110.5 s shows the highest power as a red area, and magenta equivalent current dipoles are clustered in the same region. (f) The proportion of power of the ictal onset zone relative to the whole head identified by intracranial video-electroencephalography (IVEEG) or the epileptic zone identified by intraoperative electrocorticography can be calculated from 109.5 to 110.5 s. De: delta band (0.5–3 Hz), Th: theta band (4–7 Hz), Al: alpha band (8–13 Hz), Be: beta band (14–30 Hz), LG: low gamma band (26–45 Hz), HG: high gamma band (46–70 Hz), LH: low HFO band (71–100 Hz), MH: middle HFO band (101–200 Hz), HH: high HFO band (FR, 201–330 Hz).

estimated the ECD at the spike peak. We evaluated the location of the ECD cluster and epilepsy lesion.

Determining the resection area

We determined the resected area as the epileptic focus, including the lesion, based on IVEEG or intraoperative

ECoG. We performed IVEEG for more precise seizure localization or functional mapping in cases in which the lesion was close to the eloquent area. The IVEEG electrodes consisted of subdural and strip electrodes and additional depth electrodes if necessary. In patients who underwent IVEEG, we analyzed the ictal onset zone and high power at > 50 Hz. We then superimposed the GMOT images and ECDs into the IVEEG pictures based on anatomical indicators (Sylvian fissures, central sulci, and other sulci). We then evaluated the spatial similarity between the area detected by GMOT and the ictal onset zones using IVEEG.

Seizure outcome

We applied the Engel classification to evaluate seizure outcomes at the last outpatient visit as follows: Class I, free of disabling seizures; Class II, rare disabling seizures; Class III, worthwhile improvement; and Class IV, no worthwhile improvement[4]. We compared the GMOT findings with those of ECDs and IVEEG with respect to the epileptic focus and seizure outcome.

Statistical analysis

We also used MATLAB R2020b for the statistical analyses. Fisher's exact test was used to determine the proportion of category variables. To test the proportion of a sensor's power at each band frequency relative to the whole head, we performed an arcsine transformation of the data and two-way analysis of variance (ANOVA) followed by Bonferroni correction for multiple analyses. The level of significance was set at $p < 0.05$.

RESULTS

Clinical profiles

We included 15 patients who underwent preoperative MEG and resection surgery. Table 1 describes the clinical profiles of these 15 patients, and Table 2 describes the EEG and MEG findings. The age of seizure onset ranged from 2 months to 38 years (median 14.0 years). The duration of seizures ranged from 10 months to 40 years (median 9.0 years). The age of the patients at surgery ranged from 1 to 53 (median 20.0 years). Seizure types consisted of focal aware seizure (FAS) in five patients, focal impaired awareness seizure (FIAS) in 11 patients, focal to bilateral tonic-clonic seizure (FBTCS) in three patients, and absence of atypical seizure (AAS) in one patient[7]. Three patients (cases 2, 5, and 6) had previously undergone glioma resection. SVEEG captured seizures in 12 of the 15 patients. Seizures during SVEEGs consisted of FAS in one patient, FIAS in nine patients, and FBTCS in two patients. All ictal EEGs revealed a single focal ictal discharge. Single focal interictal discharges were found in nine patients and bilateral interictal epileptiform discharges in two patients. Ten patients (cases 1, 2, 4, 6–11, 14) underwent intraoperative ECoG. Twelve patients had lesions in the temporal lobe, two had lesions in the frontal lobe, and one had a lesion in the parietal lobe. All patients underwent resective surgery, including lesions and surrounding epileptic cortices, based on intraoperative ECoG and/or IVEEG results. If the hippocampus showed spikes on the intraoperative ECoG during temporal lobe surgery, we resected the hippocampus to ensure postoperative seizure freedom (cases 7, 8, 9, 11, 12, 14, and 15). Postoperative pathological findings included glioma in eight patients (ganglioglioma, two; diffuse astrocytoma, four; oligodendroglioma, one; and anaplastic oligodendroglioma, one), cavernous hemangioma in four, focal cortical dysplasia type II in two, and dysembryoplastic neuroepithelial tumor in one patient[15]. Preoperative MEG was performed from 0.6 to 13.8 months (median 4.9 months) prior to focal resection surgery around the same time that SVEEG was performed. The postoperative clinical follow-up period ranged from 3 to 37 months (median 21.0 months). Postoperative seizure outcome of Engel class I occurred in 13 of 15 patients (87%) and class II in two of 15 patients (13%).

MEG findings

Twelve patients showed spikes on both MEG and scalp EEG. Two patients showed spikes on MEG only in the normal frequency band of 3–35 Hz without appearing on the simultaneous EEG (cases 2 and 9). ECDs clustered around the lesions in nine of the 15 patients (60%). GMOT showed high power in the FR band frequently in nine (60%) and rarely in five of 15 patients (33%). Only one of the 11 patients (9%) showed less power than 800 $(fT/cm)^2/Hz$. GMOT detected the highest power in the FR band on the brain surface around the lesions in 13 of 15 patients (87%). The area with the highest power in the FR band on GOMT coincided with the area of the ECD cluster in nine of the 15 patients (60%).

The resected area included both the ECD cluster and the area with the highest power in the FR band on GMOT in nine patients (60%). In four patients (cases 8, 11, 13, and 14), the GMOT identified the brain surface around the lesions as the area with the highest power in the FR band, although the ECDs were scattered across the bilateral hemispheres. ECD estimation and GMOT analysis did not show significant differences in the detection of epileptic foci ($p = 0.39$).

Comparison between GMOT and IVEEG

Five patients (cases 3, 5, 12, 13, and 15) underwent IVEEG before resection for further identification of the detailed resection area and functional mapping. In these five cases, the area with the highest power in the FR band by GMOT also showed high power at > 50 Hz by IVEEG. In cases 3, 12, 13, and 15, the ictal onset zone detected by IVEEG included the area with the highest power in the FR band by GMOT (Figure 3). In case 5, the ictal onset zone detected by IVEEG had a distance of one gyrus from the area with the highest power in the FR band on GMOT (Figure 4).

Proportion of power relative to the whole head

The epileptic foci in the FR band had a median proportion of power relative to the whole head of 0.0220 (0.0104–0.0887), 0.0247 (0.0101–0.0916),

Table 1 Patient clinical profiles.

No	Sex	Age (years)		Duration (years)	Seizure types	Pathology	Follow-up (months)	Engel classification
		at seizure onset	at surgery					
1	F	21	22	1	FAS	CH	36	I
2	F	20	43	23	FAS, FIAS	DA	37	I
3	M	2 m	1	10 m	FIAS	GG	33	I
4	M	17	18	1	AAS, FBTCS	DA	36	I
5	M	25	42	17	FAS	AO	31	I
6	M	14	33	19	FIAS, FBTCS	DA	9	I
7	F	4 m	6	5	FIAS	DA	21	I
8	M	6 m	11	10	FAS	OG	17	I
9	M	38	47	9	FIAS, FBTCS	CH	33	I
10	M	2	8	6	FIAS	FCD II	34	II
11	F	9	17	8	FIAS	GG	12	I
12	F	13	53	40	FIAS	CH	14	I
13	M	3	20	17	FIAS	FCD II	14	II
14	F	23	32	9	FIAS	DNT	6	I
15	M	15	18	3	FAS, FIAS	CH	3	I

F: female, M: male, m: months, AAS: atypical absence seizure, FAS: focal aware seizure, FBTCS: focal to bilateral tonic-clonic seizure, FIAS: focal impaired awareness seizure, AO: anaplastic oligodentroglioma, CH: cavernous hemanigioma, DA: diffuse astrocytoma, DNT: dysembryoplastic neuroepithelial tumor, FCD II: focal cortical dysplasia type II, GG: ganglioglioma, OG: oligodentroglioma.

Table 2 Comparison of EEG and MEG findings.

No	Video-EEG findings			MEG findings		Locations of lesions
	Seizure type	Ictal EEG fidnings	Locations of interictal epileptiform discharges	ECD detected at 3–35 Hz	GMOT detected at 201–330 Hz	
1	No seizure	None	None	Lt.T	Lt.T (Frequent)	Lt. mid T
2	FIAS	Repetitive spike and waves over Lt. T	Lt. T	Scatter	None	Lt. inf T
3	FIAS	Rythmic slow activities over Rt.T&C	Rt.C	Rt.C	Rt.C (Frequent)	Rt. pre C
4	No seizure	None	Rt. T	Lt.T	Rt.T (Rare)	Lt. sup T
5	FBTCS	Rythmic spike-and-wave over Lt. P	None	Lt.P, T	Lt.F (Rare)	Lt. sup F
6	No seizure	None	Rt.F	Rt.T	Rt.T (Frequent)	Rt. mid T
7	FIAS	Rythmic spike and waves over Rt. C	Rt.C, Lt.C	Rt.T	Rt.T (Frequent)	Rt. mid T
8	FAS	Rythmic spike and waves over Rt.T	Rt. F & T	Scatter	Rt.T (Frequent)	Rt. mid T
9	FIAS	Rythmic slow activities over Rt. F&T	None	Rt.T	Rt.T (Rare)	Rt. inf T
10	FIAS	Fast activities over Rt. T	Rt. T	Rt.T	Rt.T (Frequent)	Rt. sup T
11	FIAS	Rythmic slow activities over Rt. T	None	Scatter	Rt.T (Rare)	Rt. mid T
12	FIAS	Rythmic slow activities over Lt. F&T	Lt.T	Lt.T	Lt.T (Frequent)	Lt. mid T
13	FIAS	Fast activities over Lt. P	Rt. & Lt. O	Scatter	Lt.P (Rare)	Lt. sup P
14	FIAS	Rythmic slow activities over Lt. T	Lt.T	Scatter	Lt.T (Frequent)	Lt. inf T
15	FBTCS	Repetitive spike and waves over Rt. T	Rt.T	Rt.T	Rt.T (Frequent)	Rt. sup T

FAS: focal aware seizure, FBTCS: focal to bilateral tonic-clonic seizure, FIAS: focal impaired awareness seizure, EEG: electroencephalogram, C: central, F: frontal, Lt: left, O: occipital, P: parietal, Rt: right, T: temporal, MEG: magnetoencephalography, ECD: equivalent current dipole, GMOT: gradient magnetic-oscillation topography, AO: anaplastic oligodentroglioma, CH: cavernous hemanigioma, DA: diffuse astrocytoma, FCD II: focal cortical dysplasia type II, GG: ganglioglioma, OG: oligodentroglioma, inf T: inferior temporal gyrus, mid T: middle temporal gyrus, pre C: precentral gyrus, sup F: superior frontal gyrus, sup T: superior temporal gyrus.

0.0281 (0.0130–0.0946) at 71–100, 101–200, and 201–330 Hz, respectively. Two-way ANOVA, in which the independent variables included the case number and frequency band, showed a significant difference between the three bands ($p < 0.0001$). A Bonferroni corrected post-hoc t-test showed significant differences between 71–100 and 101–200 Hz ($p = 0.0004$), 101–200 and 201–330 Hz ($p < 0.0001$), and 71–100 and 201–330 Hz ($p < 0.0001$; Figure 5).

DISCUSSION

Summary of findings

We enrolled 15 patients with lesions who had undergone focal resection surgery for intractable epilepsy. Postoperative seizure outcomes were Engel class I in 13 of the 15 patients (87%) and Engel class II in two patients (13%). ECDs in the normal frequency band clustered around the lesions in 10 of 15 cases (66%). GMOT

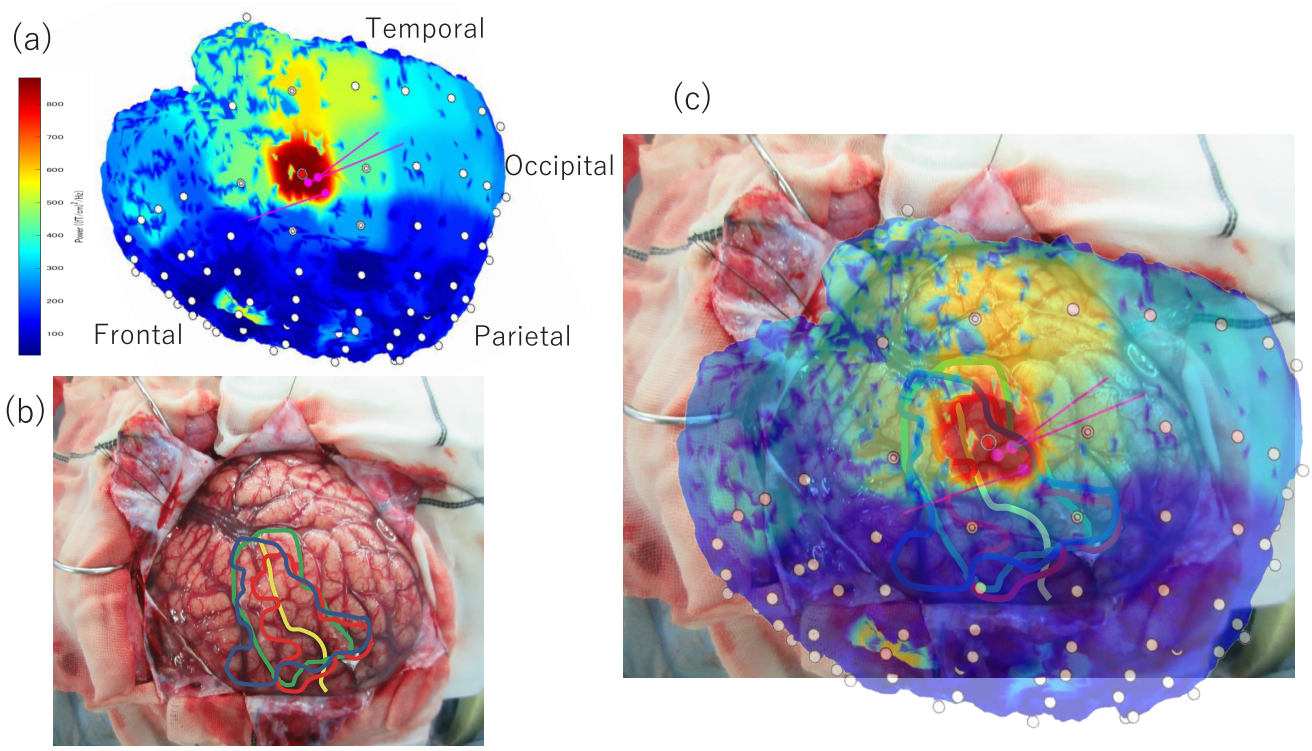

Figure 3 Findings from case 3. (a) GMOT findings over 200 Hz and dipole clustering in the deep postcentral gyrus around the ganglioglioma. Each dot indicates the projected sensor points. The red area indicates power > 800 (fT/cm)^2/Hz, and the red dot indicates the highest power. (b) An operative view of the right hemisphere with IVEEG findings; blue line: ictal onset zone at 1–50 Hz; green line: resection area; red line: highest power over 50 Hz[23]; yellow line: central sulcus. (c) A fusion of the operative view with the IVEEG findings. The red dot indicates the highest power on GMOT projected around the central sulcus.

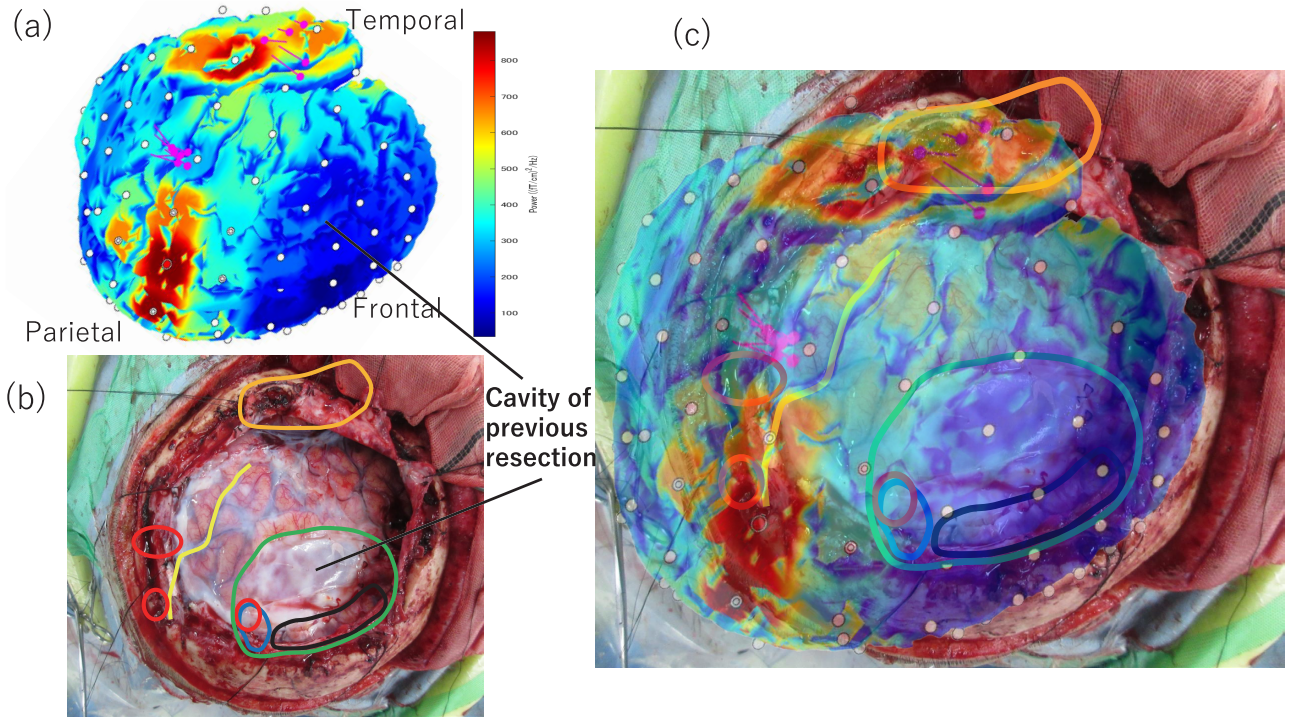

Figure 4 Findings from case 5. (a) GMOT findings over 200 Hz and dipole clustering in the left postcentral sulcus and left anterior temporal lobe. Each dot indicates the projected sensor points. The red area indicates power > 800 (fT/cm)^2/Hz, and the red dot indicates the highest power. (b) An operative view of the right hemisphere with IVEEG findings; blue line: ictal onset zone at 1–50 Hz; green line: resection area; red line: highest power over 50 Hz; yellow line: central sulcus; orange line: active interictal zone; black line: early spreading. (c) A fusion of the operative view with the IVEEG findings. The red dot indicates the highest power on GMOT projected on the left central sulcus where IVEEG also indicates high power over 50 Hz.

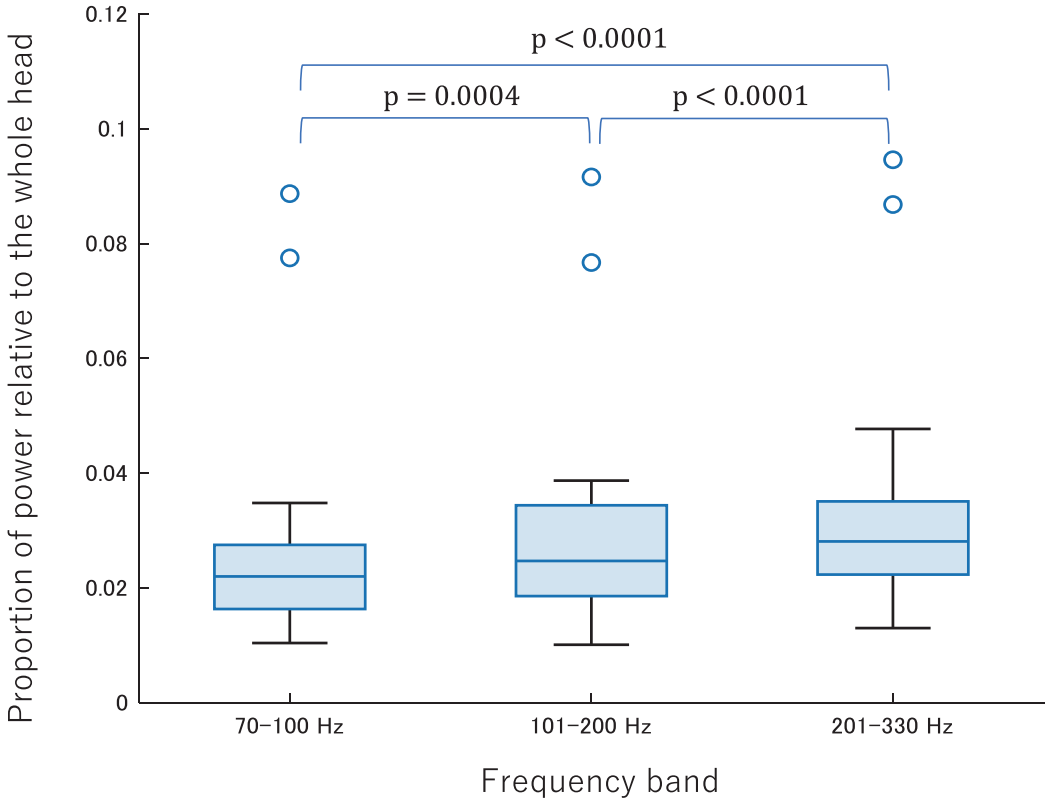

Figure 5 The proportion of power relative to the whole head of the three bands at the area detected by GMOT. Two-way analysis of variance showed significant differences in the three bands ($p < 0.0001$). A Bonferroni correction for multiple analysis showed significant differences between 71–100 and 101–200 Hz ($p = 0.0044$), 101–200 and 201–330 Hz ($p = 0.0003$), and 71–100 and 201–330 Hz ($p < 0.0001$).

detected the highest power on the brain surface in the FR band around the lesions in 13 of the 15 cases (87%). The resected area included both clustered ECDs and the highest power in the FR band on GMOT in nine of the 15 patients (60%). In five patients who underwent IVEEG, the area with the highest power at the FR band on GMOT also showed high power at > 50 Hz on IVEEG. The proportion of power in the ictal onset zone or epileptic zone significantly increased as the frequency band increased in the HFO band on the MEG ($p < 0.0001$).

The power of HFOs visualized by GMOT

Visual assessment of MEG waves is the primary method used to analyze MEG data in the normal frequency band, similar to EEG data. However, it is time-consuming to visually inspect MEG waves in the HFO band containing ten times or more waves than the normal frequency. Therefore, time-frequency analysis, which fractionates the data into short periods and analyzes the power at each, could represent an alternative method for analyzing MEG data at the HFO band[1]. Recent HFO analysis of MEG data integrates time-frequency analysis and an adaptive beamformer to construct virtual sensors of subdural electrodes[12,26]. However, adaptive beamformer-based analysis is inevitably contaminated by bias and arbitrariness because examiners must define the time range, signal space, and direction of electrodes to construct virtual sensors[12,21].

We developed the GMOT to visualize the power of all sensors directly on the brain surface without examiner bias or loss of power. The characteristics of planar gradiometers justify the assumption that the positions of the signal sources are perpendicular to the sensors[10,11]. We applied a singular-value decomposition filter to remove sensor noise. Unlike the complicated epilepsy signal, simple sensor noise may fall off during the extraction of the principal component. However, other filters may also increase the sensor-to-noise ratio[5,22]. Further accumulation of data is required to refine the selection of the most optimal filter for analyzing HFOs.

Conventional time-frequency analysis often uses spectrograms to visualize the power of each sensor[23]. Such a visualization is convenient because the signal origin is assumed to be attached to the grid of the scalp/subdural EEG. However, MEG does not allow simple power visualization because it assumes the position of the signal origin in a more complicated way. Our MEG system has unique planar gradiometer sensors that justify the assumption that the positions of the signal sources are perpendicular to the sensors[10]. This characteristic enabled us to develop the GMFT for temporal-spatial analysis[11]. Herein, we developed GMOT for time-frequency analysis to visualize the power of all planar gradiometers directly on the brain surface without examiner bias or signal loss. GMOT solves the problem of an adaptive beamformer or arbitrariness in constructing a covariance matrix[21].

ECD estimation and GMOT at the FR band

Statistical differences in performance were not found when determining the epileptic focus between ECD estimation in the normal frequency band (3–35 Hz) and GMOT analysis in the FR band (201–330 Hz). Our findings also showed that 13 of the 15 patients (87%) had high power in the FR band around their lesions. In particular, in cases 8, 11, 13, and 14, in which the ECDs were scattered across the bilateral hemispheres, GMOT analysis at the FR band provided additional information regarding laterality. Thus, searching for epileptic activity in the FR band could offer a complementary method to MEG, the conventional method of which is to detect spikes in the normal frequency band.

The power at the FR band related to the epileptic focus

The resected area had a statistically higher proportion of power relative to the entire head as the frequency band increased from 70 to 330 Hz. Classification of HFOs as FR (> 200 Hz) or ripple (< 200 Hz) cannot distinguish epileptic activity from physiological activity[2]. However, MEG analysis using an adaptive spatial filter showed that FR was most closely related to the epileptogenic zone[26]. We only enrolled patients with lesions who underwent focal resection surgery for intractable epilepsy to ensure the reliability of the epileptic focus[20,25]. The epileptic focus may have higher power, specifically in the FR band, than other brain regions. Our empirical threshold was 800 $(fT)^2/Hz$, which was derived from empty room data. High power at the FR band on the GMOT may reflect epileptic activity rather than physiological activity in patients with intractable epilepsy with lesions.

Limitations and future directions

This study had several limitations. (1) The number of cases was limited. (2) The proportion of power was only evaluated for frequency bands > 70 Hz. The normal frequency band (< 50 Hz) contained interictal discharge power that varied by case, and our power supply noise required a notch filter at 60 Hz, which could extinguish a considerable amount of the brain signal around that frequency. (3) We developed a GMFT/GMOT for our MEG system with planar gradiometers. At present, there are no data to support the application of this method to other systems. (4) The duration of the seizure outcome evaluation was not uniform.

Further studies to assess a greater number of cases and to improve our analysis are warranted. Moreover, a non-lesional study using GMOT at the FR band based on seizure outcomes is warranted.

CONCLUSION

We visualized the high power in the FR band on the brain surface. The areas of highest power in the FR band were correlated with epileptic focus based on IVEEG and intraoperative ECoG. The epileptogenic zone may have a higher power, specifically in the FR band on MEG.

Conflict of interest

We have no conflicts of interest to declare.

(Received November 28, 2022)
(Accepted February 13, 2023)

REFERENCES

1. Akiyama, T., Otsubo, H., Ochi, A., Galicia, E.Z., Weiss, S.K., Donner, E.J., et al. 2006. Topographic movie of ictal high-frequency oscillations on the brain surface using subdural EEG in neocortical epilepsy. Epilepsia 47: 1953–1957.
2. Blanco, J.A., Stead, M., Krieger, A., Stacey, W., Maus, D., Marsh, E., et al. 2011. Data mining neocortical high-frequency oscillations in epilepsy and controls. Brain 134: 2948–2959.
3. Carrette, E. and Stefan, H. 2019. Evidence for the role of magnetic source imaging in the presurgical evaluation of refractory epilepsy patients. Front. Neurol. 10: 933.
4. Engel, J. Jr, Van Ness, P.C., Rasmussen, T.B. and Ojemann, L.M. 1993. Outcome with respect to epileptic seizures. In: Engel J, Jr. Surgical Treatment of the Epilepsies. 2nd ed. Raven Press, 609–621.
5. Fan, Y., Dong, L., Liu, X., Wang, H. and Liu, Y. 2020. Recent advances in the noninvasive detection of high-frequency oscillations in the human brain. Rev. Neurosci. 32: 305–321.
6. Fisher, R.S., Webber, W.R., Lesser, R.P., Arroyo, S. and Uematsu, S. 1992. High-frequency EEG activity at the start of seizures. J. Clin. Neurophysiol. 9: 441–448.
7. Fisher, R.S., Cross, J.H., D'Souza, C., French, J.A., Haut, S.R., Higurashi, N., et al. 2017. Instruction manual for the ILAE 2017 operational classification of seizure types. Epilepsia 58: 531–542.
8. Fujiwara, H., Greiner, H.M., Lee, K.H., Holland-Bouley, K.D., Seo, J.H., Arthur, T., et al. 2012. Resection of ictal high-frequency oscillations leads to favorable surgical outcome in pediatric epilepsy. Epilepsia 53: 1607–17.
9. Gummadavelli, A., Wang, Y., Guo, X., Pardos, M., Chu, H., Liu, Y., et al. 2013. Spatiotemporal and frequency signatures of word recognition in the developing brain: a magnetoencephalographic study. Brain Res. 1498: 20–32.
10. Hämäläinen, M., Hari, R., Ilmoniemi, R.J., Knuutila, J. and Lounasmaa, O.V. 1993. Magnetoencephalography—theory, instrumentation, and applications to noninvasive studies of the working human brain. Rev. Mod. Phys. 65: 413–497.
11. Hashizume, A., Iida, K., Shirozu, H., Hanaya, R., Kiura, Y., Kurisu, K., et al. 2007. Gradient magnetic-field topography for dynamic changes of epileptic discharges. Brain Res. 1144: 175–179.
12. Hillebrand, A., Singh, K.D., Holliday, I.E., Furlong, P.L. and Barnes, G.R. 2005. A new approach to neuroimaging with magnetoencephalography. Hum. Brain Mapp. 25: 199–211.
13. Iida, K., Otsubo, H., Matsumoto, Y., Ochi, A., Oishi, M., Holowka, S., et al. 2005. Characterizing magnetic spike sources by using magnetoencephalography-guided neuronavigation in epilepsy surgery in pediatric patients. J. Neurosurg. 102: 187–196.
14. Kagawa, K., Iida, K., Hashizume, A., Katagiri, M., Baba, S., Kurisu, K., et al. 2016. Magnetoencephalography using gradient magnetic field topography (GMFT) can predict successful anterior corpus callosotomy in patients

with drop attacks. Clin. Neurophysiol. 127: 221–229.
15. Louis, D.N., Perry, A., Reifenberger, G., von Deimling, A., Figarella-Branger, D., Cavenee, W.K., et al. 2016. The 2016 World Health Organization Classification of Tumors of the Central Nervous System: a summary. Acta Neuropathol. 131: 803–820.
16. Nagarajan, S.S., Attias, H.T., Hild, K.E. 2nd and Sekihara, K. 2006. A graphical model for estimating stimulus-evoked brain responses from magnetoencephalography data with large background brain activity. Neuroimage 30: 400–416.
17. Okamura, A., Otsubo, H., Hashizume, A., Kagawa, K., Katagiri, M., Seyama, G., et al. 2020. Secondary epileptogenesis on gradient magnetic-field topography correlates with seizure outcomes after vagus nerve stimulation. Epilepsy Res. 167: 106463.
18. Otsubo, H., Ochi, A., Imai, K., Akiyama, T., Fujimoto, A., Go, C., et al. 2008. High-frequency oscillations of ictal muscle activity and epileptogenic discharges on intracranial EEG in a temporal lobe epilepsy patient. Clin. Neurophysiol. 119: 862–868.
19. Papadelis, C., Tamilia, E., Stufflebeam, S., Grant, P,E., Madsen, J.R., Pearl, P.L., et al. 2016. Interictal high frequency oscillations detected with simultaneous magnetoencephalography and electroencephalography as biomarker of pediatric epilepsy. J. Vis. Exp. 118: 54883.
20. Rosenow, F. and Lüders, H. 2001. Presurgical evaluation of epilepsy. Brain 124: 1683–1700.
21. Sekihara, K., Nagarajan, S.S., Poeppel, D., Marantz, A. and Miyashita, Y. 2001. Reconstructing spatio-temporal activities of neural sources using an MEG vector beamformer technique. IEEE Trans. Biomed. Eng. 48: 760–771.
22. Sekihara, K., Nagarajan, S.S., Poeppel, D., Marantz, A. and Miyashita, Y. 2002. Application of an MEG eigenspace beamformer to reconstructing spatio-temporal activities of neural sources. Hum. Brain Mapp. 15: 199–215.
23. Shimoyama, I., Kasagi, Y., Kaiho, T., Shibata, T., Nakajima, Y. and Asano, H. 2000. Flash-related synchronization and desynchronization revealed by a multiple band frequency analysis. Jpn. J. Physiol. 50: 553–559.
24. Sueda, K., Takeuchi, F., Shiraishi, H., Nakane, S., Sakurai, K., Yagyu, K., et al. 2013. Magnetoencephalographic analysis of paroxysmal fast activity in patients with epileptic spasms. Epilepsy Res. 104: 68–77.
25. Téllez-Zenteno, J.F., Hernández Ronquillo, L., Moien-Afshari, F. and Wiebe, S. 2010. Surgical outcomes in lesional and non-lesional epilepsy: a systematic review and meta-analysis. Epilepsy Res. 89: 310–318.
26. Velmurugan, J., Nagarajan, S.S., Mariyappa, N., Mundlamuri, R.C., Raghavendra, K., Bharath, R.D., et al. 2019. Magnetoencephalography imaging of high frequency oscillations strengthens presurgical localization and outcome prediction. Brain 142: 3514–3529.
27. Xiang, J., Korman, A., Samarasinghe, K.M., Wang, X., Zhang, F., Qiao, H., et al. 2015. Volumetric imaging of brain activity with spatial-frequency decoding of neuromagnetic signals. J. Neurosci. Methods 239: 114–128.